Vol.8 No.4
Autumn 1997

EXTENSION OF LINEAR ISOTHERM REGULARITY TO LOWER DENSITY RANGE*

B. Najafi and G. Parsafar

College of Chemistry, Isfahan University of Technology, Isfahan, 84154, Islamic Republic of Iran

Abstract

The general equation of state which was found for dense fluids, both compressed liquids and dense supercritical fluids, namely "Linear Isotherm Regularity," is extended to the lower density range, specifically for densities lower than the Boyle density. This new equation of state which is called "ELIR" is shown to be compatible with the equations of state based on statistical-mechanical theory, although ELIR gives a more accurate density at high pressures. This equation of state has been tested with experimental data for different fluids (Ar, N_2, O_2, CO, CH_4, C_3H_8, CH_3OH, H_2) for both vapor and compressed liquid phases. The ELIR is able to predict the critical isotherm and also both of the coexistence phases at equilibrium can be expressed by a single ELIR equation of state.

Introduction

The quest for a simple analytical equation of state for fluids is very old, the van der Waals equation is the first real attempt. In the early 1990's, two very successful new equations of state were developed. The first one based on statistical-mechanical perturbation theory which was developed by Ihm-Song-Mason has been very successful for fluids at low densities ($\rho < 1.4\ \rho_B$, where ρ_B is the Boyle density) [1]. The second one, which is called "Linear Isotherm Regularity" and abbreviated as "LIR", was derived by Parsafar and works very well for fluids at high densities ($\rho > \rho_B$) [2]. According to LIR, $(Z-1)v^2$ varies linearly with respect to ρ^2, where $Z \equiv \frac{p}{\rho RT}$ is the compression factor and $\rho \equiv \frac{1}{v}$ is the molar density. LIR has also been used to predict the known regularities and some new ones as well [3,4]. LIR was tested with experimental data for different fluids, including monatomic, polyatomic, hydrocarbons, alcohols, and polar fluids, and it was shown that LIR is compatible with the equations of state based on statistical-mechanical theory, although the latter do not predict as great a range of linearity as suggested by experiment [5].

In a previous article [5], it was shown that LIR works for densities greater than the Boyle density and for temperatures below about twice the Boyle temperature. The main goal of this paper is to extend LIR for densities below the Boyle density. The Boyle temperautre T_B and Boyle volume v_B are defined in terms of the second virial coefficient B_2 as follows: $B_2(T_B)= 0$ and $v_B= T_B B'_2(T_B)$, where $B_2 = \frac{dB_2}{dT}$. The Boyle density, $\rho_B \equiv \frac{1}{v_B}$, is about 1.8 ρ_c [5].

Keywords: Critical region; Equation of state; Extended linear isotherm regularity; Phase transition

*This paper is dedicated to Professor E.A. Mason.

Extension of the LIR to Low Density Range

The LIR is simply written as

$$(Z - 1)v^2 = A + B\rho^2 \qquad (1)$$

where A and B are two temperature dependent parameters which depend on the type of fluid.

The total potential energy among N molecules, U, is given by [5],

$$\frac{U}{N} = \frac{K_n}{v^{n/3+1}} - \frac{K_m}{v^{m/3+1}} \qquad (2)$$

where K_n and K_m are constants. Using the above equation along with the exact thermodynamic relation

$$p = T\left(\frac{\delta p}{\delta T}\right)_\rho - \left(\frac{\delta E}{\delta V}\right)_T$$

where E is internal energy, one can obtain the following result [5],

$$(Z-1)\,v^2 = -\frac{A}{RT}\rho^{\frac{m}{3}-1} + \frac{B_1}{RT}\rho^{\frac{n}{3}-1} + \frac{1}{\rho^2}\left[\frac{1}{\rho R}\left(\frac{\delta p}{\delta T}\right)_\rho - 1\right] \qquad (3)$$

where A_1 and B_1 are constants. In order to model the experimental results, it is taken that m= 3 and n= 9 and the last term is nearly constant, which is replaced by A_2, an approximation which is reasonable only at high densities. The final result was found to be

$$A = A_2 - \frac{A_1}{RT} \quad \text{and} \quad B = \frac{B_1}{RT} \qquad (4)$$

For the low density range, the last term in Equation 3, A_2, cannot be assumed to be constant any more. In order to find A_2 in terms of temperature and density, we use the van der Waals fluid model. Using the van der Waals EOS, Equation 3 can be written as

$$(Z-1)\,v^2 = -\frac{A_1}{RT} + \frac{B_1}{RT}\rho^2 + \frac{b}{\rho}\frac{1}{1-b\rho} \qquad (5)$$

If we expand the last term of Equation 5 as a power series in density, we obtain

$$\frac{Z-1}{\rho} = \sum_{i=0} \alpha_i \rho^i \qquad (6)$$

Since at low densities Equation 6 has to follow the virial EOS, we conclude that

$$\alpha_0 = B_2$$
$$\alpha_1 = C$$

where B_2 and C are the second and third virial coefficients, respectively.

In order to find the other coefficients in Equation 6 we may require that this equation matches smoothly with Equation 1 at $\rho = \rho_B$ (LIR equation). Smooth connection can be obtained by matching two functions and their first and second derivatives at a common density, specifically the Boyle density. The final result obtained is,

$$\frac{Z-1}{\rho} = B_2 + C\rho + \alpha_2\rho^2 + \alpha_3\rho^3 + \alpha_4\rho^4 \qquad (7)$$

where

$$\alpha_2 = \frac{3}{\rho_B}(A - C) - \frac{6B_2}{\rho_B^2}$$

$$\alpha_3 = -\frac{3}{\rho_B^2}(A - C) + \frac{8B_2}{\rho_B^3} + B$$

$$\alpha_4 = \frac{1}{\rho_B^3}(A - C) - \frac{3B_2}{\rho_B^4}$$

in which A and B are the LIR parameters, Equation 1, B_2 and C are the virial coefficients, and ρ_B is the Boyle density. The final EOS given by Equation 7 will be called the Extended Linear Isotherm Regularity or simply "ELIR" from now on. As we noted, LIR is an accurate EOS for $\rho \geq \rho_B$ and ELIR for $\rho < \rho_B$.

Experimental Section

In this section, we examine the accuracy of the calculated results obtained from ELIR, first for subcritical and supercritical fluids (by supercritical we mean $T>T_c$), and then the fluids around the critical region.

a- Subcritical and Supercritical Fluids

Nitrogen serves as our primary test fluid because of the abundance of experimental p-v-T data [6]. ELIR (EOS) has five parameters, their values are given for N_2 at different temperatures in Table I and for different fluids in Table II. Using the experimental data, the values of A and B parameters at any temperature may be obtained from the intercept and slope of $(Z-1)v^2$ versus ρ^2 for that isotherm, respectively. The experimental values of the second and third virial coefficients are tabulated in the literature [7].

To see the accuracy of ELIR, we have calculated nitrogen density for different isotherms at given pressures.

The results are summarized in Table I, including the intercept, A, and slope, B, of the fitted straight line $(Z-1)v^2$ versus ρ^2 for $\rho \geq \rho_B$, and the second and third virial coefficients for N_2 for given pressure range, Δp. Also, the average absolute percent deviation of the calculated density is given for each isotherm. The maximum deviations are given in parentheses.

In order to see whether ELIR is limited to a certain type of fluid or is generally true, we have calculated the density for one subcritical and one supercritical isotherm of different fluids. The average absolute percent deviation of the calculated density, compared to the experimental values [8-12], is given for each fluid in Table II which includes monatomic, polar, nonpolar, hydrogen bonded, and quantum fluids. We may conclude that ELIR can be used to calculate the density of all types of fluids, both for the subcritical and supercritical isotherms, with a maximum deviation of a few percent.

Comparison of ELIR with ISM Equation of State

Equations of state based on statistical-mechanical perturbation theory are available and ELIR can be compared with them. The ELIR may be compared with an accurate EOS based on statistical-mechanical perturbation theory modified by a new strong principle of corresponding states, namely ISM equation of state [1]. This EOS can be written in a form analogous to Equation 7 as

$$\frac{Z-1}{\rho} = \frac{\alpha}{1-\lambda b\rho} - \frac{\alpha - B_2}{1+\delta b \rho}$$

where B_2 is the second virial coefficient, α is a temperature-dependent parameter that scales for the softness of the repulsive forces, and b is a temperature-dependent parameter analogue of the van der Waals covolume related to α. The constants δ and λ are characteristic of the particular fluid.

The experimental compression factor of CH_4 at 500 K [10] is compared with the calculated values given by ELIR and ISM equations of state at this temperature, as shown in Figure 1. Although the results of ELIR and ISM equations of state are in good agreement with the experimental data at low densities, at high densities the values given by ELIR are closer to the experimental data than ISM. It is well known that ISM is more accurate at low densities, while significant deviations occur in the high density range (for $\rho > 1.4\rho_B$) [5]. A similar comparison is made for some other fluids given in Table III, for which the average absolute percent deviation of the calculated density for the typical isotherms is calculated.

b-Critical Region

In this section, we shall investigate the accuracy of the predicted densities given by ELIR for fluids in the vicinity of the critical temperature. The calculated Z is plotted versus ρ in Figure 2 for argon at 150 K, in which the experimental data [8] and the results given by the ISM equation of state [1] are included for comparison.

As for the subcritical and supercritical fluids presented in the previous section, both ELIR and ISM equations of state give very accurate results at low densities. However,

Table I. Intercept (A) and slope (B) of $(Z-1)v^2 = A + B\rho^2$, the second and third virial coefficients, the pressure range (Δp) of the data, and the average absolute percent deviation of the calculated density at a given temperature for nitrogen*

T	$A*10^3$	$B*10^6$	B_2*10^3†	$C*10^6$†	ΔP	$100(\Delta\rho/\rho)_{ave}$
K	L^2mol^{-2}	L^4mol^{-4}	$L\ mol^{-1}$	$L^2\ mol^{-2}$	MPa	
120	-5.4614	8.5818	-118.0	2890	0.02-3	0.42(1.4)
200	-1.3240	5.5800	-36.1	1940	.02-50	0.50(1.7)
300	0.89611	3.4338	-4.76	1405	.02-100	0.30(0.9)
400	1.8261	2.3840	8.94	1146	.02-100	0.42(1.8)
500	2.2573	1.7813	16.39	988	.02--150	1.10(2.8)
600	2.5847	1.2788	21.31	950	.02-150	0.60(2.2)
700	2.6562	1.0470	23.92	1197	.02-250	1.31(4.1)
800	2.8378	.70612	25.98	1444	.02-300	1.42(4.2)

*Data from Ref. 6. Maximum deviations are given in parentheses.
Boyle density is 20 mol Lit^{-1}.
†Ref. 7

Table II. Same as Table I, for different fluids (subcritical and supercritical)

Fluid	T	$A*10^3$	$B*10^6$	B_2*10^3†	$C*10^6$†	ρ_B	ΔP	$100(\Delta\|\rho\|\rho)_{ave}$
	K	L^2mol^{-2}	L^4mol^{-4}	L mol^{-1}	L^2 mol^{-2}	mol L^{-1}	MPa	
Ar[a]	120	-5.2857	4.8790	-133.1	2170	24.0	0.08-1	0.16.(23)
Ar[a]	300	-0.0734	2.0174	-15.70	1120	24.0	0.08-1	0.20(1.1)
O_2[b]	120	-4.8300	4.1280	-139.9	2187	22.8	0.10-5	0.23(1.1)
O_2[b]	300	-0.1072	2.1592	-15.90	1149	22.8	0.1-70	0.10(0.3)
CO[b]	273	-0.4402	4.4311	-13.60	1378	20.0	0.1-90	0.10(0.6)
CH_4[c]	155	-9.1781	1.5059	-168.0	3720	18.0	.025-1	0.25(0.4)
CH_4[c]	300	-1.6050	7.7286	-41.49	2355	18.0	.025-80	0.82(2.9)
CH_4[c]	500	1.4243	4.1374	-0.5	1462	18.0	.01-160	0.20(0.7)
H_2O[d]	473	-2.1436	0.7428	-209.0	-23000	31.7	.01-1.4	0.06(0.3)
CH_3OH[e]	500	-6.8458	1.4360	-178.7	-7590	15.5	.01-6	0.66(1.2)
H_2[b]	90	0.30747	0.48613	-5.54	663.5	28.4	0.1-20	0.41(0.9)
C_3H_8[b]	360	-27.260	220.64	-256.8	13000	9.18	0.1-6.5	1.10(4.7)
C_3H_8[b]	500	-11.351	169.10	-124.0	22390	9.18	0.01-35	1.60(5.2)

[a]Ref. 8, [b]Ref. 9, [c]Ref. 10, [d]Ref. 11, [e]Ref. 12
†Data from Ref. 7

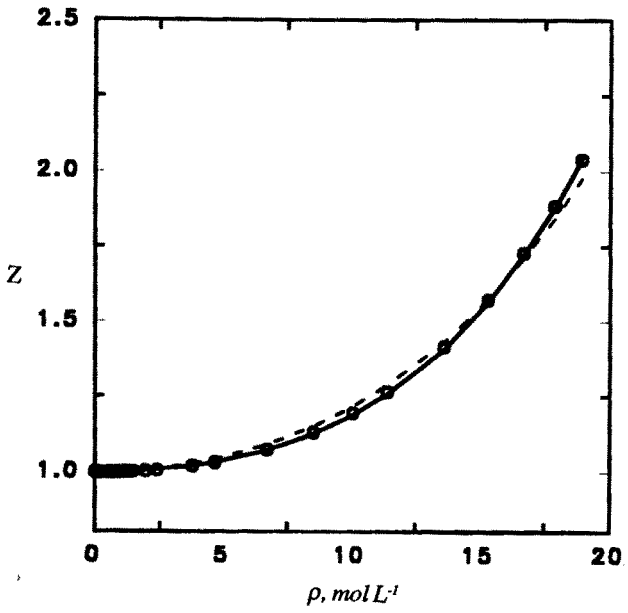

Figure 1. Experimental compression factor (O) of CH_4 at 500 K is compared with the calculated values given by the ELIR (solid curve) and the ISM (dashed curve)

both equations disagree somewhat with experiment at intermediate densities (mainly around the critical density). Such disagreement is no surprise, because it is known that the critical region is nonanalytic [1, 13], and is not expected to be predicted by any analytical EOS. As shown in Figure 2, the ISM gives a significant deviation in the high density region at T_c, in which the ELIR gives a very accurate result. A similar calculation is carried out for different fluids, for which the results are given in Table IV.

Two-Phase Region

Any subcritical isotherm of a real fluid shows a first order phase transition, at which density changes suddenly. However, there is no analytical EOS by which the transition can be predicted [1]. The calculated pressure given by ELIR versus density is plotted in Figure 3 for some given isotherms of argon. As is shown in this figure, ELIR predicts a van der Waals loop for each isotherm with $T<T_c$, a difficulty which is observed by many analytical equations of state. The vapor pressure can, nevertheless, be predicted by applying the Maxwell-equal-area construction to the loops. By increasing

Table III. The average absolute percent deviation of the calculated density given by the ELIR and ISM in comparison with the experimental data for different fluids

Fluid	T,K	$100(\Delta\|\rho\|/\rho)_{ELIR}$	$100(\Delta\|\rho\|/\rho)_{ISM}$	Δp, MPa
N_2[a]	200	0.50(1.7)	0.48(2.1)	.02-40
N_2[a]	300	0.30(0.9)	0.65(6.2)	.02-100
N_2[a]	600	0.60(2.2)	1.94(9.6)	.15-200
Ar[b]	120	0.16(.23)	0.02(0.7)	.08-1.5
Ar[b]	300	0.20(1.1)	1.11(3.8)	.08-100
CH_4[c]	155	0.25(.40)	0.02(.16)	.025-1
CH_4[c]	500	0.20(.70)	1.15(2.2)	.10-140

[a]Ref. 6, [b]Ref. 8 [c]Ref. 10

Table IV. Same as Table I, for different fluids (subcritical and supercritical)

Fluid	T	A*10³	B*10⁶	B_2*10³†	C*10⁶†	ΔP	$100(\Delta\|\rho\|/\rho)_{ELIR}$	$100(\Delta\|\rho\|\rho)_{ISM}$
	K	L^2mol^{-2}	L^4mol^{-4}	L mol^{-1}	L^2 mol^{-2}	MPa		
N_2[a]	126	-4.9630	8.2546	-103.3	3345	0.08-8	1.3(9)	3.3(13)
Ar[b]	150	-3.4658	3.9610	-85.80	2360	0.1-8	1.8(10)	8.3(73)
O_2[c]	155	-3.3207	3.7519	-85.90	2423	.1-10	1.9(15)	—
CH_4[d]	190	-6.0046	11.987	-116.3	4741	.01-8	6.0(19)	10(40)

[a]Ref. 6, [b]Ref. 8, [c]Ref. 9, [d]Ref. 10
Maximum deviations are given in parentheses.
†Ref. 7

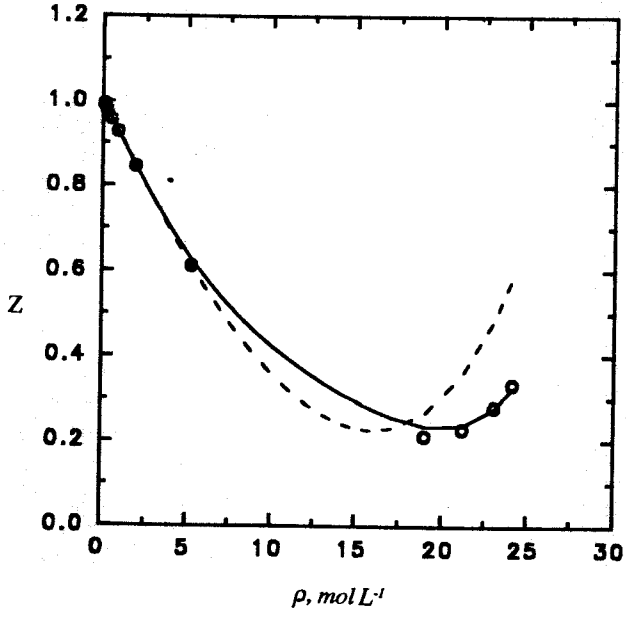

Figure 2. Same as Figure 1 for argon but for the critical isotherm

temperature, the metastable phase (the loop) reduces to a flat inflexion at T_c.

However, the ELIR accurately predicts the stable branches of p-ρ isotherms, for both the vapor and the compressed liquid, (Fig. 3).

p-T Isochores (Isometrics)

For real fluids, the curves of constant density in a p-T plot (isochores) are nearly linear, a fact that impressed the earliest investigators of fluid compressibility [14]. Any sensible equation of state must thus give nearly linear isochores. On closer inspection, the isochores of real fluids will show small negative curvatures (concave downwards) at both low and high densities. The general experimental situation is less clear at intermediate densities, but at least a number of the lower hydrocarbons show a region of small positive curvature [15].

The isochores of the van der Waals equation are all linear, those of the Dieterici equation all show positive curvature, and those of the Beattie-Bridgeman and Redlich-Kwong equations all show negative curvature. Only the eight-parameter equation of Benedict, Webb, and Rubin

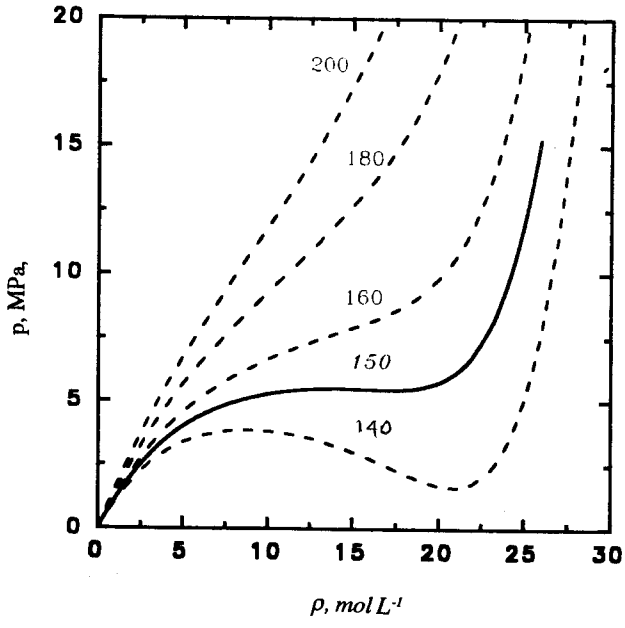

Figure 3. Pressure versus density calculated by ELIR for given isotherms of argon. The flat inflexion appears for the critical isotherm (solid curve). The numbers present the temperature in Kelvin.

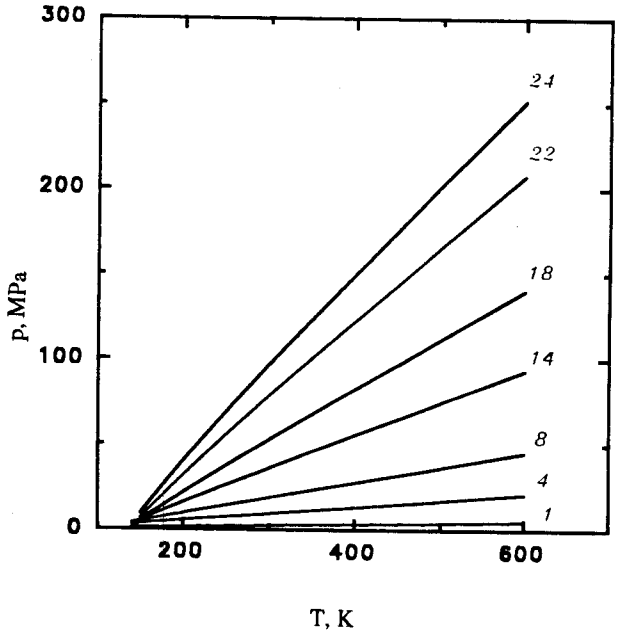

Figure 4. Pressure versus temperature for different isochores of argon calculated by the ELIR, the numbers present the density in moles per liter.

manages to shift from negative to positive and back to negative curvature as the density increases [13].

LIR predicts a linear relation for p versus T for each isochore of dense fluids, when $\rho \geq \rho_B$. The line goes through the origin when $\rho = \rho_{0z}$, where ρ_{0z} is the density of the common compression point [3].

Since the temperature dependency of the virial coefficients are not known, analytically, it is impossible to obtain p as an explicit function of T from ELIR, for isochores, however, it is possible to plot p against T for each isochore, numerically. The results are shown in Figure 4 for argon. This figure shows a small concave (negative curvature) for isochores at high densities, in such a way that it becomes significant for densities close to the Boyle density. For the low density range, in which the van der Waals EOS is more realistic, we may use the analytical form for the virial coefficients given by vdw EOS as

$$B_2 = b - \frac{a}{RT} \quad \text{and} \quad C = b^2$$

where, a and b are the van der Waals parameters. If we substitute $A = A_2 - \frac{A_1}{RT}$ and $B = \frac{B_1}{RT}$ (see Ref. 5) into Equation 7 and express $Z = \frac{pv}{RT}$ into ELIR, we shall find the following result:

$$p = f(\rho) + g(\rho)T$$

where $f(\rho)$ and $g(\rho)$ are some functions of density. Therefore, it is expected that the ELIR gives a straight line for p versus T for each isochore at low density. This expectation is in accordance with the results given in Figure 4.

Results and Discussion

The existence of a common equation of state for dense fluids, namely LIR, and also another common equation of state for compressed solids [16] reveals the fact that almost a common short range effective pair interaction potential governs among particles in dense fluids (when $\rho \geq \rho_B$) and solids. In spite of the fact that the ELIR represents a general EOS for less compressed fluids, ($\rho < \rho_B$), and because of the fact that the potential energy involves both directly (via volume) and indirectly (via the virial coefficients), in this equation of state, we may conclude that the effective long range interaction potential depends on the molecular properties of the fluid.

Such a conclusion may be expected, because of the fact that the long range interactions become important in the less dense fluid. The effective interaction pair potential may be divided into three different molecular separation ranges. At a very short range on the repulsive wall, the potential may be given by $V = V_0 \exp(-r/\rho)$, where V_0 and

ρ are the energy and range parameters respectively [17]. At intermediate separation around the minimum of the potential well, the effective pair potential may be given by LJ (12,6) [5]. However, in the long range region, in which the dominant potential depends on the type of intermolecular forces (dipole-dipole, dipole-induced-dipole, dipole-quadropole,...), for instance for the noble gas the long range potential may be given as [17],

$$V = -\frac{C_6}{r^6} - \frac{C_8}{r^8} - \frac{C_{10}}{r^{10}}$$

Therefore, a general analytical expression for the potential does not exist. By noting that for $\rho > \rho_B$ the dominant portion of the potential is around the bottom of the potential well, and for $\rho < \rho_B$, is in the long range portion of the potential, the universality form of LIR and the dependency of ELIR on the virial coefficients are reasonable.

The results given by the ELIR are compared with both experiment and the Ihm-Song-Mason EOS. We found that ELIR gives a better agreement with experiment, specially at high density range (Fig. 2).

Finally, in comparison with the more commonly used Tait-Murnaghan equation (TME) [5] and the recently introduced equation of state by Baonze *et al.* (BE) [18], the LIR and ELIR equations of state can be easily used to calculate other thermodynamic properties, and also their parameters can be easily calculated because of the abundance of accurate p-v-T data and the virial coefficients.

Also these two equations of state together cover the whole density range of fluid, while TME and BE equations are valid only at high densities and the ISM equation at low densities.

Acknowledgements

We wish to thank the Isfahan University of Technology Research Council for financial support.

References

1. Ihm, G., Song, Y. and Mason, E.A. *J. Chem. Phys.*, **94**, 3839, (1991).
2. Parsafar, G. A. *J. Sci. I.R. of Iran.*, **2**, 111, (1991).
3. Najafi, B., Parsafar, G. A. and Alavi, S. *J. Phys. Chem.*, **99**, 9248, (1995).
4. Alavi, S., Parsafar, G.A. and Najafi, B. *International Journal of Thermophysics*, **16**, 1421, (1995).
5. Parsafar G.A. and Mason, E.A. *J. Phys. Chem.*, **97**, 9048 (1993).
6. Jacobsen, R. T., Stewart, R. B. and Jahangiri, M. *J. Phys. Chem. Ref. Data*, **15**, 735, (1986).
7. Dymond, H. and Smith, E. B. *The virial coefficients of pure gases and mixtures. A critical compilation.* Oxford University Press, London, (1980).
8. Stewart, R. B. and Jacobsen, R. T. *J. Phys. Chem. Ref. Data*, **18**, 639, (1989).
9. Vargaftik, N. B. *Handbook of physical properties of liquids and gases*, (2nd edn), (English translation). Hemisphere, New York, (1983).
10. Younglove, B. A. and Ely, J. E. *J. Phys. Chem. Ref.* Data, **16**, 577, (1987).
11. Van Wylen, G. J. and Sonntag, R. E. Fundamentals of classical thermodynamics, (2nd edn.) John Wiley and Sons, Inc., (1976).
12. Goodwin, R. D. *J. Phys. Chem. Ref.* Data, **16**, 799, (1987).
13. Song, Y. and Mason, E.A. *J. Chem. Phys.*, **91**, 7840, (1989).
14. Beattie, J.A. and Stockmayer, W. H. *Ref. Prog. Phys.*, **7**, 195 (1940).
15. Beattie, J. A. and Stockmayer, W. H. States of matter. In *Treatise on physical chemistry*, Vol. **2**, Chap. 2, (3rd edn) (ed. H.S. Taylor and S. Glasstone). Van Nostrand, New York, (1951).
16. Parsafar, G. A. and Mason, E. A. *Physical Review B*, **49**, 3049, (1994).
17. Najafi, B., Mason, E. A. and Kestin J. *Physica*, **119A**, 387, (1983).
18. Baonza, V. G., Caceres, M. and Nunez, J. *J. Phys. Chem.* **97**, 10813, (1993).